Journal of Alloys and Compounds 769 (2018) 539–544

Contents lists available at ScienceDirect

Journal of Alloys and Compounds

journal homepage: http://www.elsevier.com/locate/jalcom

Magnetic behavior of Fe nanoparticles driven by phase transition of FeF_3

Tsuyoshi Takami [a, *], Keitaro Matsui [b, 1], Hiroshi Senoh [b], Noboru Taguchi [b], Masahiro Shikano [b], Hikari Sakaebe [b], Toshiharu Fukunaga [a]

[a] Office of Society-Academia Collaboration for Innovation, Center for Advanced Science & Innovation, Kyoto University, Gokasho, Uji, Kyoto 611-0011, Japan
[b] Research Institute of Electrochemical Energy (RIECEN), National Institute of Advanced Industrial Science and Technology (AIST), 1-8-31 Midorigaoka, Ikeda, Osaka 563-8577, Japan

ARTICLE INFO

Article history:
Received 22 May 2018
Received in revised form
2 August 2018
Accepted 4 August 2018
Available online 7 August 2018

Keywords:
Magnetism
ADF-STEM
Fe nanoparticles
Fluoride
Phase transition

ABSTRACT

Typical electrodes for Li-ion batteries such as $LiCoO_2$ operate via the insertion/de-insertion of Li ions; innovative electrodes that undergo conversion reactions have been developed to meet the requirement for greater capacities. However, batteries operating via a conversion process suffer from degradation over repeated cycles and from hysteresis in charge/discharge profiles, and their mechanism remains a topic of ongoing debate. We prepare the FeF_3/C composite electrode as a model electrode to address the conversion mechanism. Magnetization measurements provide direct evidence of superparamagnetic behavior—Fe nanoparticles (NPs) are magnetized similarly to a paramagnet under an external field—-after the discharge process. We quantify the size of the Fe NPs, and find a correlation between an increased Fe particle size and a decrease in discharge capacity. These findings would pave the strategy based on control of the size of Fe NPs for realizing a favorable cycling performance. Indeed, improvement of an electrolyte goes toward higher capacities after 30 cycles.

1. Introduction

Reducing the dependence of modern society on fossil fuels is one of the urgent issues. In the path toward a greener and more sustainable society, electric-energy storage using battery is a key technology. Lithium (Li)-ion batteries with higher volumetric and gravimetric energy densities have enabled the realization of environmentally benign power storage from super-slim microchips to lap-top computers. Considering the ever-growing demand for electric vehicles and grid energy storage applications on a larger scale, important is an increase in density of the stored energy, which is the product of voltage and capacity, beyond that of existing Li-ion batteries.

Classical electrodes for Li-ion batteries operate via the insertion/de-insertion of Li ions. $LiCoO_2$, for example, serves as the cathode in rechargeable batteries that packed a lot of energy into a small, lightweight package. The insertion/de-insertion reaction basically involves at most one electron per 3d-metal; two or more electrons per redox center can be involved in the following conversion reaction: $M_xX_y + ne^- + nLi^+ \rightleftarrows xM + yLi_mX$, where $m = n/y$ ($n \geq 2$), M = Fe, Co, Ni, etc.; X = F, O, S, etc. The conversion reaction results in the formation of M and Li_mX; that is, a phase transition from the initial M_xX_y compound to M and Li_mX takes place during the discharging process, and vice versa during the charging process. For example, the electrochemical activities for X = F and O have been reported by Arai et al. [1] and Tarascon's group [2], respectively. These conversion cathodes promise an enhanced capacity compared with insertion-based cathodes; however, conversion batteries face technical challenges related to their degradation over cycles (poor cycling stability) and a marked hysteresis in their charge/discharge profiles, which remain formidable hurdles for their further application.

The FeF_3 cathode (M = Fe and X = F; $x = 1$ and $y = 3$) [1], which exhibits the highest theoretical capacity ($712\ mA\,h\,g^{-1}$) among the fluorides of M = Fe, Co, Ni, and Cu, experiences two stages of insertion/de-insertion and conversion reactions [3–6]:

$$FeF_3 + Li^+ + e^- \rightleftarrows LiFeF_3 (\text{or } FeF_2 + LiF), \tag{1}$$

$$LiFeF_3 (\text{or } FeF_2 + LiF) + 2Li^+ + 2e^- \rightleftarrows 3LiF + Fe. \tag{2}$$

---

* Corresponding author.
E-mail address: t-takami@saci.kyoto-u.ac.jp (T. Takami).

[1] Present address. Murata Manufacturing Co. Ltd., 2288, Ohshinohara, Yasu-shi, Shiga 520-2393, Japan.

https://doi.org/10.1016/j.jallcom.2018.08.040
0925-8388/© 2018 Elsevier B.V. All rights reserved.

In the initial discharge process represented by Eq. (1), the Li ions are accommodated in the interstitial sites in FeF_3 maintaining its original crystal structure. When more Li ions are introduced into the lattice, a phase transition to LiF and Fe occurs according to the conversion process shown in Eq. (2). It remains controversial whether the intermediate phase is $LiFeF_3$ or a mixture of FeF_2 and LiF. Electrochemically driven Fe nanoparticles (NPs) are believed to promote the electrochemical activity. In the simple binary metal fluorides FeF_2 and CuF_2, the morphology and distribution of cationic species (Fe and Cu) are indeed key factors in the reversibility of the conversion reaction [7,8]. The Fe NPs are interconnected and form a bicontinuous network, with Li being mobile, resulting in the reversible charge/discharge profile; the larger Cu NPs are isolated from the LiF phase, resulting in an irreversible charge/discharge profile [7,8]. In addition to the existence of the Fe NPs in a FeF_2 system, their size has been quantified after the selected cycles, 1st and 20th cycles, from high-resolution transmission electron microscopy (TEM) [9]. While most of the studies on the conversion mechanism have been devoted to the simple metal (II) fluorides, to our knowledge not much work has been performed on the complex Fe(III) fluoride.

Reinvigorated by these studies, we focus on the Fe(III) fluoride with the highest capacity and clarify the conversion mechanism for the FeF_3 cathode, in particular what size of Fe NPs are produced and how they are distributed upon cycling. The lack of such fundamental understanding hinders the rational design of cathode materials and batteries. Senoh et al. investigated the degradation mechanism of the conversion-type FeF_3/C composite, in which FeF_3 with a low electronic conductivity was synthesized with carbon, by synchrotron X-ray diffraction (XRD), X-ray absorption near edge structure, extended X-ray absorption fine structure, and total scattering measurements [10]; however, the above information has not yet been fully derived. For example, the XRD peaks corresponding to Fe became broad and overlapped with the peaks of LiF, which makes it difficult to determine the size of Fe NPs. Since superconducting quantum interference device (SQUID) magnetometer has proved useful for describing the character of magnetic NPs [11–13], for example, in our previous study [11], we derived information on the size and distribution of Co NPs by the coercivity and remanence ratio obtained by magnetic measurements. In the present study, we systematically examined the magnetic properties after charge/discharge cycles with the goal of addressing the above issues and clarifying mainly how Fe NPs and the resulting discharge profile are intertwined.

2. Experimental

2.1. Sample preparation

The FeF_3/C composite was synthesized by combining the FeF_3 powder (Rare Metallic Co., Ltd.) and acetylene black (Denka Co., Ltd.) in a weight ratio of 70:25. The powder mixture was placed in a steel container with zirconia bowls, and milling was performed for 24 h using a planetary ball mill (Premium Line P-7, Fritsch) at 200 rpm. The cathode was prepared by mixing the FeF_3/C composite powder and polyvinylidene difluoride (Kureha Chemical Industries) with N-methyl-2-pyrrolidone (Kishida Chemical Co., Ltd.) in a weight ratio of 95:5. This slurry was coated onto a piece of aluminum foil as a current collector. The resulting FeF_3/C composite electrode was dried at 363 K for at least 12 h under vacuum to achieve complete evaporation of the solvent. The cathode disks with a projected area of 1.77 cm^2 were fabricated by punching from the FeF_3/C composite electrode.

2.2. Charge/discharge measurements

Coin-type cells were assembled using Li metal foil as the anode, polypropylene separators, and 1 mol dm^{-3} $LiPF_6$ or $LiBF_4$ in 1:1 v/v ethylene carbonate (EC) and 1,2-dimethyl carbonate (DMC) as the electrolyte. Galvanostatic charge and discharge measurements started with a charge process at 298 K. The cut-off voltages were 1.0 and 4.5 V for the discharge and charge profiles, respectively, at a current density corresponding to 0.05C. Here, nC means that the current will charge or discharge the full capacity in $1/n$ h.

2.3. Magnetization and ADF-STEM measurements

Magnetization was measured *ex situ* using a SQUID magnetometer (Magnetic Property Measurement System MPMS-7, Quantum Design, Inc.). The cells were disassembled under an argon atmosphere inside a glove box, and the samples were subsequently collected by scraping the powder mixture from the current collectors at various states after the charge/discharge measurements. The samples were sealed in quartz tubes (ϕ 5 mm $\times \approx$ 15 mm) with Araldite® to avoid exposure to air. We adjusted the magnetic field (1 kOe) so that the particle size determined by using a SQUID magnetometer is consistent with that done by XRD and TEM. Annular dark-field scanning transmission electron microscopy (ADF-STEM) measurements were performed using a $TITAN^3$ G2 60-300 (FEI) operated at 120–300 kV. The samples were transferred to the electron microscope from an Ar-filled glove box without exposure to air.

3. Results and discussion

3.1. Charge-discharge profile

Fig. 1 shows the charge/discharge profile of the FeF_3/C composite electrode at 298 K over 30 cycles. At the initial stage, our FeF_3 cathode exhibited a specific capacity of approximately 600 mA h g^{-1} (84% of the theoretical value), which is 3–5 times larger than that of the $LiCoO_2$ cathode (120–180 mA h g^{-1}) [14]. The initial capacity is somewhat smaller than that reported by Li et al. [15], but the practical capacity per weight of our FeF_3/C composite electrodes is larger due to high ratio of FeF_3 in the composite electrode. The voltage plateaus in the discharge curves at approximately 3.2 V and below 1.8 V are assigned to the insertion reaction of FeF_3 to $LiFeF_3$ (or FeF_2 + LiF) (Eq. (1)) and the conversion reaction of $LiFeF_3$ (or FeF_2 + LiF) to LiF and Fe (Eq. (2)), respectively. Both the charge and discharge capacities were prone to decreasing as cycling

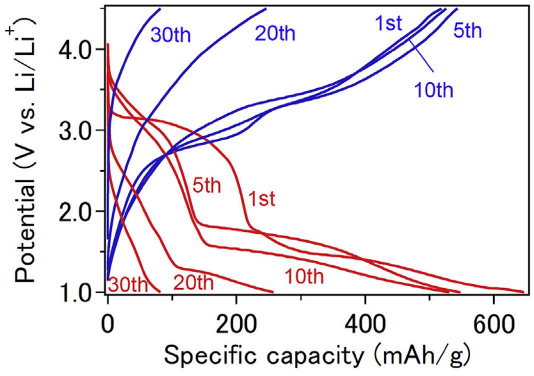

Fig. 1. Charge (blue) and discharge (red) profiles for the FeF_3/C electrode at 298 K over 30 cycles. (For interpretation of the references to colour in this figure legend, the reader is referred to the Web version of this article.)